Published in final edited form as:
J Mol Neurosci. 2010 January ; 40(1-2): 77–86. doi:10.1007/s12031-009-9261-0.

Tricks of Perspective: Insights and Limitations to the Study of Macroscopic Currents for the Analysis of nAChR Activation and Desensitization

Roger L. Papke
Department of Pharmacology and Therapeutics, College of Medicine, University of Florida, P.O. Box 100267, Gainesville, FL 32610-0267, USA

Abstract

Activation, inactivation, and desensitization are key features of ion channel behavior. We endeavor to understand these processes at the level of the single molecules and extrapolate from such microscopic models the behavior of ion channels in contexts of cellular physiology and therapeutics. In the case of ligand-gated ion channels, such as nicotinic acetylcholine receptors (nAChRs), it is also important to consider the nature of the dynamic changes in the chemical stimulus required for activation. The amplitude and time course of the agonist pulse provided to nAChR at a fast synapse will be vastly different from those of the ACh stimulus presented to presynaptic receptors in the brain and neither of these physiological processes will resemble the stimuli presented by nicotine self-administration or with systemic delivery of a therapeutic agent. Likewise, specific experimental protocols will provide unique stimulus profiles, which will impact the relationship between the macroscopic data and the underlying molecular processes. In this work, ion channel simulations intended to model heteromeric neuronal nAChR are conducted under varying conditions of agonist presentation, and the impact of a key microscopic process, desensitization, is studied on the macroscopic responses. With instantaneous jumps in agonist concentrations, the microscopic desensitization rate impacts essentially all aspects of the macroscopic responses, rise rates, decay rates, and both peak and steady-state currents. In contrast, with an agonist pulse like that used in *Xenopus* oocyte experiments, microscopic desensitization rates have a profound impact on peak current amplitude and very little effect on the kinetics of the macroscopic responses.

Keywords

nAChR; Activation; Desensitization

Introduction

As scientists, we must accept the fact that the nature of our data is in part determined by the way we make our measurements, and it is incumbent on us to be mindful of the limitations imposed by our experimental methods. Under the best of circumstances, we endeavor to match our experimental perspectives to some sort of “real world” condition. As biologists, we seek to study physiologically relevant conditions, and as bio-medical scientists, we want

rlpapke@ufl.edu .

Proceedings of the XIII International Symposium on Cholinergic Mechanisms

to understand how drugs will function under therapeutically relevant conditions. In the case of drugs targeting endogenous neurotransmitter systems such as nicotinic acetylcholine receptors (nAChR), we need to address both physiological and therapeutic perspectives on receptor activation and desensitization.

Our earliest perspective on nAChR came from the postsynaptic membrane of neuromuscular junctions (NMJs), beginning with the work of Bernard Katz and his co-workers (Fatt and Katz 1951; del Castillo and Katz 1957). The elaboration of that perspective, with the study of post-synaptic currents, the significance of cholinesterase function (Land et al. 1984), and, ultimately, detailed descriptions of single-channel currents (Colquhoun and Sakmann 1985), has given us a rich literature and a view of nAChR as mediators of synaptic function. However, the perspective of nAChR that came from studies of the NMJ is of limited value for understanding the functional dynamics of nAChR in the brain, especially in regard to how they respond to self-administered nicotine or drugs that would be used therapeutically.

The physiologically important behavior of nAChR occurs under non-stationary conditions (Jones and Westbrook 1996). Under physiological conditions prior to activation in the absence of agonist, receptors are in a resting state (R). When the resting receptors are exposed to a rapid and transient increase in the concentration of agonist (A), an equally rapid and largely synchronous activation of receptors occurs. If the presence of agonist is prolonged, the majority of the receptors convert to a desensitized state (D). However, the effect of ACh at the NMJ is very short-lived because of the highly localized expression of acetylcholine esterase (AChE). This perspective, established by studies of the NMJ, allowed us to directly relate endplate currents to quantitative knowledge of receptor density, single-channel activation kinetics, ACh quantal content, the spatial relationship between ACh release sites and the receptors, transmitter diffusion, and the kinetics of ACh metabolism (Land et al. 1984).

Unfortunately, almost none of what we know about synaptic transmission at the NMJ can be applied directly to the function of nAChR in the brain. There is scant evidence that brain nAChR mediate fast synaptic transmission and vastly more evidence that they modulate synaptic function mediated by other neurotransmitters (Glisson et al. 1972; Wonnacott et al. 1989; Role and Berg 1996; Albuquerque et al. 1997, 2009; Radcliffe et al. 1999; Ji et al. 2001). In the brain, nAChR are found predominantly on presynaptic terminals and at perisynaptic sites on dendrites. Even when nAChR have been demonstrated to be present on nerve cell bodies, their expression appears to be diffuse over the cell surface and not associated with either pre-or post-synaptic specializations (Roth et al. 2000; Buhler and Dunwiddie 2002; Frazier et al. 2003; Thinschmidt et al. 2005). While there are well-defined cholinergic pathways in the brain, such as the pathway from the medial septum into the hippocampus, electrical stimulation of that pathway does not appear to produce point-to-point synaptic transmission via nAChR. But rather, ACh seems to be released diffusely and subsequently binds to the various populations of presynaptic, perisynaptic, and somatic receptors (Descarries et al. 1997).

We must therefore develop an appropriate perspective for understanding the physiological functions of nAChR in the brain and beyond that, a perspective on how nicotine or potential therapeutic agents, delivered systemically and metabolized far more slowly than ACh, will operate on the nAChR of the brain. Two issues will be key to these crucially needed new perspectives; firstly, we need to establish a better understanding of how the kinetics of transmitter (or drug) delivery affects both receptor activation and desensitization, and secondly, we need to consider models that encompass both non-stationary and steady-state aspects of receptor activation in balance with desensitization. Furthermore, we need to

resolve these issues with perspectives that can be provided by the available experimental methods.

In this work, simulated data based on a classic model for nAChR activation and desensitization (del Castillo and Katz 1957) are presented. By imposing limitations on that model that are consistent with a standard experimental approach, transformations of the simulated data are generated that are consistent with experimental results. This transformation provides an informative perspective on the relationship between idealized models of receptor function based on microscopic rate constants and macroscopic currents generated under experimentally and therapeutically relevant conditions.

Methods

Simulations

Single and multichannel simulations were conducted with the SIMU module (version 2.0.0.337) of QUB (Qin et al. 1997) provided by Tony Auerbach and co-workers (State University of New York at Buffalo, Buffalo, NY). Simulations of instantaneous responses were based on the summed activity of 1,000 channels with a time interval of 10 μs. Simulation of responses to agonist pulses were the summed activity of 10,000 channels at a time interval of 50 μs.

The output from the simulations were saved as text files and then imported into pClamp (version 9.2, Molecular devices, Union City, CA) for subsequent analysis and graphic export of sample traces. The multi-segment option of SIMU was used to generate multiple independent data sets for statistical comparisons when necessary.

Representative data from oocytes expressing human α4β2 nAChR were recorded with OpusXpress as previously reported (Papke and Papke 2002). The cDNA clones were generously provided by Dr. Jon Lindstrom (U. Penn, Philadelphia, PA).

Results

The Simulation of Macroscopic Current Responses with a Linear Model

The general equation for an ion channel mediated response is $I=(E_M-E_R)NP_o\gamma$, where I is the current, (E_M-E_R) is the electrical driving force, calculated as the difference between the holding potential (E_M) and the reversal potential (E_R) for the ion channel being studied, N is the total number of channels, P_o is the percentage of channels opened (or the probability of any single channel being open), and γ is the conductance of a single channel. The simulations allow for both γ and N to be fixed and, based on the rate constants selected, determine how P_{open} will vary as a function of time and stimulus. The simulation accepts an initial condition with all of the channels in a resting state and agonist concentration at zero. The system can then be perturbed by applying an instantaneous jump in agonist concentration. A simple representation of such a non-stationary perturbation is shown in Fig. 1. If the agonist concentration (A) is assumed to jump effectively instantaneously to a concentration high enough to saturate the binding sites, then the model can be reduced to transitions between the three agonist-occupied states. Current will depend on both N (fixed) and P_{open} (which will vary over time), but it is important to note that essentially identical currents can arise when N is high and the maximum P_{open} is low as when the reverse is true. In order to illustrate this, we can take the most idealized case where backward rates from AR* to AR and AD to AR are essentially zero. For the model on the left, we assign a relatively fast opening rate and a slow desensitizing rate, while for the model on the right, those rates are reversed.

In this highly simplified example, the macroscopic current responses represent the product of just two first-order processes, activation and desensitization. Since we think about the processes of activation and desensitization as occurring in a sequential manner, it is an appealing, albeit invalid, assumption to associate the rise in current to the activation process and the decay in current to desensitization (or inactivation). However, the macroscopic responses of both the rapidly activating and the slowly activating channels are described by a fast exponential rise rate and an exponential decay rate that is in both cases slower than the rise rate. The kinetics of desensitization in one case dominates the rising phase and in the other case the falling phase. This is because the rise rates reflect whatever is the fastest process. In order for macroscopic currents simulated for the low P_{open} channels on the right to have the same peak amplitude as for the high P_{open} channels on the left, the model must simply assume a larger total number of low P_{open} channels.

However, it will be noted that simulated currents of the low P_{open} channel have greater variance around what would be the mean of multiple measured currents than do the currents of the high P_{open} channels. This is especially evident in the relatively low amplitude currents (Fig. 1, bottom-most traces). This relationship between mean current amplitude and variance in non-stationary ion channel currents has been used experimentally to obtain estimates of both P_{open} and N from macroscopic currents under conditions when neither P_{open} was very small nor N was very large (Traynelis et al. 1993).

Simulations of ACh-Evoked Responses with a Cyclic Model and Instantaneous Jumps in Agonist Concentration

The model in Fig. 2 is largely based on the Katz and Thesleff cyclic model for nAChR activation and desensitization (Katz and Thesleff 1957). The model is simplified relative to our current understanding by condensing two agonist binding events to a single step. The rate constants are consistent with single-channel data for heteromeric neuronal nAChR (Papke et al. 1989). Single-channel simulations with this model (not shown) generate mean channel open times of 0.5 ms and bursts with probability of 0.57 for reopening at non-saturating concentrations of agonist and clusters of bursts at saturating concentrations of agonist (Colquhoun and Ogden 1988). Intercluster closed times were approximately 10 ms. Equilibrium desensitization of receptors in the absence of agonist is 1%, and the affinity of agonist for the desensitized state is 300-fold higher than for the resting state of the receptor. Simulated macroscopic currents for 1,000 channels to instantaneous jumps at the indicated ACh concentrations are shown on the right in Fig. 2a. At ACh concentrations ≥10 μM, the currents are biphasic with an initially high P_{open} that decays to a steady-state level, as channels go back and forth between activatable and desensitized states.

Figure 2b shows the concentration–response curves for both peak and steady-state currents generated by this model, with instantaneous steps in agonist concentration. With large jumps in ACh concentrations, peak P_{open} values plateau at approximately 0.60 with an EC_{50} of 25 μM. However, as shown in the representative traces (Fig. 2a), with high ACh concentrations the peak P_{open} is reached rapidly and P_{open} rapidly falls to a steady-state level of approximately 0.10. Interestingly, the EC_{50} for steady-state currents is more than an order of magnitude lower than for the generation of peak currents.

Impact of Desensitization Rates on Macroscopic Currents

As shown in Fig. 1, no simple association can be made between specific rates in a kinetic model and particular features of associated macroscopic responses, even in the most highly simplified models. Simulations with the model in Fig. 2a were conducted with adjustments in just the desensitization rate (d^+) between the AR and AD states. Several features of the macroscopic responses were altered when d^+ was decreased from 3,000 to 1,000 s^{-1} (ACh

concentration fixed at 100 μM). Both the peak and steady-state values of P_{open} are increased when the desensitization rate is decreased, and the time required to reach steady state is also increased. Likewise, when d^+ was increased from 3,000 to 10,000 s^{-1}, both the peak and steady-state values of P_{open} were decreased, and the time required to reach steady state was also decreased. There were additionally significant ($p<0.05$) effects on rise rates. When the concentration of ACh was 100 μM and d^{-1} was 1,000 s^{-1}, the time to peak current was 1.08±0.4 ms ($n=4$), and when d^{-1} was increased to 10,000 s^{-1}, the time to peak current decreased to 0.56±0.4 ms ($n=4$). As shown in Fig. 2d, there was a similar trend in the data for the effect of desensitization rate on time to peak current when ACh concentration was reduced to 10 μM. However, with the reduction in maximal P_{open}, the variation in the data was increased, and the differences were not statistically significant with $n=4$.

Changes in a single rate in this model effectively altered all of the features of the evoked responses. However, in these simulations, ACh concentration effectively increased from 0 to 100 μm in 10 μs (the time step of the simulation), a perturbation that would be considered unrealistically fast, even for the NMJ.

Simulations of ACh-Evoked Responses with Agonist Pulses

We have previously characterized the solution exchange dynamics in the *Xenopus* oocyte recording/expression system (Papke and Thinschmidt 1998). Agonist concentrations reach peak levels within a few seconds and then decay somewhat more slowly. The responses of heteromeric neuronal nAChR, such as the human α4β2 receptors illustrated in Fig. 3a, show ACh concentration-dependent increases in peak amplitude and kinetics that roughly parallel those of the solution exchange, so that concentration response relationships for peaks and net charge typically are not significantly different (Papke and Papke 2002). The model in Fig. 2 was adapted to make ACh concentrations rise and fall over the time course of seconds, similar to the conditions of an oocyte experiment. The standard agonist pulse (Fig. 3b) was generated with a rise rate of 1 s^{-1} and a washout rate of 0.25 s^{-1} (Fig. 3b), which gave a time to peak of 1.9 s and a 90% to 20% decay time of 6.6 s.

As shown in Fig. 3b, the pulse-model-generated concentration-dependent currents similar to those actually recorded from *Xenopus* oocytes (Fig. 3a). Likewise, with the ACh pulse-driven model the concentration–response relationships for net charge and peak currents, expressed relative to maximum responses, are essentially identical to each other, as is normally the case for heteromeric neuronal nAChR expressed in oocytes (Papke and Papke 2002). When the peak current responses are expressed relative to the absolute P_{open} (by dividing the number of channels open at the peak by the total number of channels in the simulation), the model gives data fit with the same EC_{50} as the data on steady-state P_{open} obtained with step changes in ACh concentration (Fig. 2b), with a maximum P_{open} value of 0.075, which is relatively close to the maximum steady-state P_{open} seen with instantaneous agonist applications

As noted above, it is a common, but erroneous, assumption that the decay rates of macroscopic currents reflect the microscopic desensitization rates of the receptors. However, as shown in Fig. 2, changes in the rate of desensitization affect virtually all aspects of the macroscopic responses to instantaneous jumps in ACh concentration. To determine which aspects of the responses to a pulse of ACh would be most sensitive to the desensitization rate, 10,000 channel simulations were run with d^+ set at 1,000 or 10,000 s^{-1}, and the results were compared to the standard condition (Fig. 3) where d^+ was set at 3,000 s^{-1}. The results (Fig. 4a) show that changing the microscopic desensitization rate in the underlying model profoundly affected the peak current amplitudes of the responses to ACh pulses but had relatively little effect on the response waveforms. While a tenfold increase in d^+ produced an 86% reduction in peak current, the kinetics of the responses was accelerated by only 13–

14%. Moreover, increased desensitization rate affected time-to-peak equally as much as it affected decay times.

The data suggest that, while responses to the agonist pulses may be valid reflections of channel behavior under steady-state conditions (as in Fig. 2), they are nearly blind to the non-stationary portions of the currents generated with instantaneous jumps in ACh concentrations. This hypothesis seems reasonable since pulses were used, which had rise times of a second or more, while with instantaneous concentration jumps, steady-state conditions were reached within 10–20 ms, even with relatively low concentrations of agonist (Fig. 2). To determine the degree to which the various features of the macroscopic responses were dependent on the speed of agonist application, additional pulseevoked simulations were conducted with the same underlying microscopic model shown in Fig. 2a, but with varying rise rates for the agonist pulse (from 0.25 to 1,024 s^{-1}), keeping the pulse decay rate constant at 0.25 s^{-1}. Note that pulses with a fast onset but slow washout would be consistent with drug application protocols commonly used in brain slice experiments, where pressure applications may generate rapid increases in drug concentration around a patch-clamped cell that are then only slowly reduced by bulk solution flow in the chamber (Lopez-Hernandez et al. 2007).

The parameters measured were time-to-peak current, net charge, 90% to 20% decay time, and peak P_{open}. The first three parameters are plotted in Fig. 4b measured relative to responses with the slowest application rate, and peak P_{open} was calculated relative to the total number of channels in the simulations (10,000). As expected, the rise times of the macroscopic currents were directly related to the application rate of the agonist pulse (Fig. 4b). Peak P_{open} and decay times were largely insensitive to application rates between 0.5 and 128 s^{-1}. However, at rates of application faster than 128 s^{-1}, the macroscopic currents became biphasic with early transient peaks (not shown) that became progressively larger with increasing application rates and resembled the transient portions of the step-current responses (Fig. 2).

Note that although the fast transient component of the currents obtained with fast applications greatly increased the peak P_{open} (and decreased the 90% to 20% decay times), there was effectively no impact of the fast transient current on the integrated net charge of the total responses (Fig. 4b).

Discussion

When Hodgkin and Huxley first described the voltage-dependent sodium currents of squid axon, they developed a model that assigned fast activation rates and relatively slow inactivation rates to the underlying molecular mediators of those currents. Although the work of those pioneering biophysicists is still held in high regard, the solution that they proposed to describe the behavior of voltage-dependent sodium channels was not a unique solution for the data. In fact, while Hodgkin and Huxley modeled sodium channel behavior to be rather like the high P_{open} channels in Fig. 1 (left), subsequent single-channel studies (Aldrich et al. 1983;Horn and Vandenberg 1984) have indicated that mammalian sodium channels, in fact, behave more like the low P_{open} channels in Fig. 1 (right). Therefore it is clear, as confirmed by the present work, that we need to be circumspect about applying what may seem to be intuitive assumptions as we try to relate macroscopic events to models of molecular behavior. In this regard, we need to consider the limitations imposed by our experimental methods and specific perspectives they provide on the data we acquire.

It remains unknown how high local concentrations of ACh become in the brain, and how fast the ACh signals reach the populations of receptors on cell bodies or presynaptic

terminals. Likewise it is unknown how long the acetylcholine signals persist until they are eliminated by metabolism or diluted by diffusion. There are high levels of AChE in the parts of the brain that are dense in cholinergic fibers, but the esterase expression is relatively diffuse and not associated with other synaptic specializations. Our general lack of knowledge about the nature of cholinergic signals presented to nAChR in the brain, and the absence of cholinergic synapses that can be readily studied in the brain, leaves us at something of a loss for how we might try to recapitulate a physiologically relevant ACh signal when we attempt to characterize heteromeric neuronal nAChR through the expression of receptors in artificial systems such as transfected cells or *Xenopus* oocytes.

One major cholinergic pathway in the CNS arises in the septum and projects into the hippocampus and other forebrain areas. Studies of the septo-hippocampal pathway indicate that it may provide oscillations in cholinergic tone associated with rhythmic firing (theta rhythms) in the range of 5–12 Hz. Coincidence or asynchrony of synaptic activity to theta rhythms is likely to be a primary determining factor for the precise neuromodulatory effects of nicotinic cholinergic receptors in the brain (Smythe et al. 1992). If release and degradation of ACh is tightly coupled to the frequency of theta rhythms, then ACh activation of neuronal nAChR may work primarily through the transient high P_{open} phases that occur with rapid and brief pulses of agonist. However, if diffusion significantly slows the delivery of ACh to the endogenous receptors, then currents mediated by channels approaching steady-state equilibrium between activation and desensitization will also be significant, especially in regard to net-charge transfer, which might mediate changes in intracellular calcium. In fact, the simulations suggest that with sustained stimuli, steady-state currents will have far more impact on net-charge transfer than transient high P_{open} currents.

While it may not be the case that endogenous ACh-mediated signals in the brain persist long enough for steady-state currents to be of greater consequence than transient currents, steady-state activity associated with an equilibrium of channels between activation and desensitization will certainly be a predominant functional mode for channel activity following the self-administration of nicotine (Picciotto et al. 2008; Rahman et al. 2008) or the systemic delivery of therapeutic drugs. In that regard, the simulations suggest that relatively slow experimental measurements, such as those obtained from *Xenopus* oocytes, should be accurate reporters of the effects of nicotine and experimental drugs on nAChR in the brain. It has been proposed from studies of receptor activation and desensitization in the nAChR-rich medial habenula that a balance between these processes produces “window currents,” which mediate the long-term effects of ACh delivered from diffuse release sites as well as the effects of self-administered nicotine (Lester 2004).

The addicting effects of nicotine are believed to be mediated primarily by β2-containing heteromeric receptors (Picciotto et al. 1998), which our simulations were intended to emulate. It should be noted that the models tested in this study do not emulate the behavior of the second main brain nAChR subtype, homomeric α7 receptors. The α7-type neuronal nAChR receptors show a unique concentration-dependent form of desensitization that is consistently manifested, regardless of whether the receptors are stimulated on a time scale of minutes or milliseconds. Models for α7 activation and desensitization have been presented and discussed elsewhere (Mike et al. 2000; Papke et al. 2000; Uteshev et al. 2002).

It should also be noted that these experiments have modeled only a rapid form of desensitization, which is most readily observed in single-channel recordings in the presence of high concentrations of ACh (Colquhoun and Ogden 1988). There is also evidence that, in the prolonged presence of agonists, and especially with prolonged exposure to nicotine, nAChR may manifest other, more long-lived forms of desensitization or inactivation (Fenster et al. 1999; Gentry and Lukas 2002; Vann et al. 2006). An understanding of the

significance of such long-lived forms of desensitization or inactivation for therapeutics or nicotine dependence might require yet another perspective than the one provided in the current experiments.

In conclusion, as we try to move from the limited perspective provided by classical studies of the NMJ to an understanding of nicotine addiction and potentially nAChR-directed therapeutics, we must remain mindful of both the strengths and limitations imposed by our methods, embrace the data obtained from different perspectives, and integrate the information thus acquired.

Acknowledgments

These studies were supported by NIH grant GM57481. The author thanks Clare Stokes, Dustin Williams and Dr. Gretchen López-Hernández for helpful comments.

References

Albuquerque EX, Alkondon M, Pereira EFR, Castro NG, Schrattenholz A, Barbosa CTF, et al. Properties of neuronal nicotinic acetylcholine receptors: Parmacological characterization and modulation of synaptic function. Journal of Pharmacology and Experimental Therapeutics 1997;280:1117–1136. [PubMed: 9067295]

Albuquerque EX, Pereira EFR, Alkondon M, Rogers SW. Mammalian nicotinic acetylcholine receptors: From structure to function. Physiological Reviews 2009;89(1):73–120. [PubMed: 19126755]

Aldrich RW, Corey DP, Stevens CF. A reinterpretation of mammalian sodium channel gating based on single channel recording. Nature 1983;306:436–441. [PubMed: 6316158]

Buhler AV, Dunwiddie TV. alpha7 nicotinic acetylcholine receptors on GABAergic interneurons evoke dendritic and somatic inhibition of hippocampal neurons. Journal of Neurophysiology 2002;87:548–557. [PubMed: 11784770]

Colquhoun D, Ogden DC. Activation of ion channels in the frog end-plate by high concentrations of acetylcholine. Journal of Physiology 1988;395:131–159. [PubMed: 2457675]

Colquhoun D, Sakmann B. Fast events in single-channel currents activated by acetylcholine and its analogues at the frog muscle end-plate. Journal of Physiology 1985;369:501–557. [PubMed: 2419552]

del Castillo J, Katz B. Interaction at endplate receptors between different choline derivatives. Proceedings of the Royal Society of London Series B 1957;146:369–381.

Descarries L, Gisiger V, Steriade M. Diffuse transmission by acetylcholine in the CNS. Progress in Neurobiology 1997;53:603–625. [PubMed: 9421837]

Fatt P, Katz B. An analysis of the endplate potential recorded with an intra-cellular electrode. Journal of Physiology 1951;115:320–370. [PubMed: 14898516]

Fenster CP, Beckman ML, Parker JC, Sheffield EB, Whitworth TL, Quick MW, et al. Regulation of alpha4beta2 nicotinic receptor desensitization by calcium and protein kinase C. Molecular Pharmacology 1999;55:432–443. [PubMed: 10051526]

Frazier CJ, Strowbridge BW, Papke RL. Nicotinic acetylcholine receptors on local circuit neurons in the dentate gyrus: a potential role in the regulation of granule cell excitability. Journal of Neurophysiology 2003;89:3018–3028. [PubMed: 12611982]

Gentry CL, Lukas RJ. Regulation of nicotinic acetylcholine receptor numbers and function by chronic nicotine exposure. Current Drug Targets—CNS & Neurological Disorders 2002;1:359–385. [PubMed: 12769610]

Glisson SN, Karczmar AG, Barnes L. Cholinergic effects on adrenergic neurotransmitters in rabbit brain parts. Neuropharmacology 1972;11:465–477. [PubMed: 4340143]

Horn R, Vandenberg CA. Statistical properties of single sodium channels. Journal of General Physiology 1984;84:505–534. [PubMed: 6094703]

Ji D, Lape R, Dani JA. Timing and location of nicotinic activity enhances or depresses hippocampal synaptic plasticity. Neuron 2001;31:131–141. [PubMed: 11498056]

Jones MV, Westbrook GL. The impact of receptor desensitization on fast synaptic transmission. Trends in Neurosciences 1996;19:96–101. [PubMed: 9054063]

Katz B, Thesleff S. A study of the "desensitization" produced by acetylcholine at the motor end-plate. Journal of Physiology 1957;138:63–80. [PubMed: 13463799]

Land BR, Harris WV, Salpeter EE, Salpeter MM. Diffusion and binding constants for acetylcholine derived from the falling phase of miniature endplate currents. Proceedings of the National Academy of Sciences of the United States of America 1984;81:1594–1598. [PubMed: 6584895]

Lester RA. Activation and desensitization of heteromeric neuronal nicotinic receptors: Implications for non-synaptic transmission. Bioorganic & Medicinal Chemistry Letters 2004;14:1897–1900. [PubMed: 15050622]

Lopez-Hernandez G, Placzek AN, Thinschmidt JS, Lestage P, Trocme-Thibierge C, Morain P, et al. Partial agonist and neuromodulatory activity of S 24795 for alpha7 nAChR responses of hippocampal interneurons. Neuropharmacology 2007;53:134–144. [PubMed: 17544457]

Mike A, Castro NG, Albuquerque EX. Choline and acetylcholine have similar kinetic properties of activation and desensitization on the alpha7 nicotinic receptors in rat hippocampal neurons. Brain Research 2000;882:155–168. [PubMed: 11056195]

Papke RL, Papke JKP. Comparative pharmacology of rat and human alpha7 nAChR conducted with net charge analysis. British Journal of Pharmacology 2002;137:49–61. [PubMed: 12183330]

Papke RL, Thinschmidt JS. The correction of alpha7 nicotinic acetylcholine receptor concentration-response relation-ships in *Xenopus* oocytes. Neuroscience Letters 1998;256:163–166. [PubMed: 9855365]

Papke RL, Boulter J, Patrick J, Heinemann S. Single-channel currents of rat neuronal nicotinic acetylcholine receptors expressed in *Xenopus laevis* oocytes. Neuron 1989;3:589–596. [PubMed: 2484342]

Papke RL, Meyer E, Nutter T, Uteshev VV. Alpha7-selective agonists and modes of alpha7 receptor activation. European Journal of Pharmacology 2000;393:179–195. [PubMed: 10771012]

Picciotto M, Zoli M, Rimondini R, Lena C, Marubio L, Pich E, et al. Acetylcholine receptors containing the beta2 subunit are involved in the reinforcing properties of nicotine. Nature 1998;391:173–177. [PubMed: 9428762]

Picciotto MR, Addy NA, Mineur YS, Brunzell DH. It is not "either/or": activation and desensitization of nicotinic acetylcholine receptors both contribute to behaviors related to nicotine addiction and mood. Progress in Neurobiology 2008;4:329–342. [PubMed: 18242816]

Qin F, Auerbach A, Sachs F. Maximum likelihood estimation of aggregated Markov processes. Proceedings of the Royal Society of London Series B, Biological Sciences 1997;264:375–383.

Radcliffe KA, Fisher JL, Gray R, Dani JA. Nicotinic modulation of glutamate and GABA synaptic transmission of hippocampal neurons. Annals of the New York cademy of Sciences 1999;868:591–610.

Rahman S, Lopez-Hernandez GY, Corrigall WA, Papke RL. Neuronal nicotinic receptors as brain targets for pharmacotherapy of drug addiction. CNS & Neurological Disorders Drug Targets 2008;7:422–441. [PubMed: 19128201]

Role L, Berg D. Nicotinic receptors in the development and modulation of CNS synapses. Neuron 1996;16:1077–1085. [PubMed: 8663984]

Roth AL, Shoop RD, Berg DK. Targeting alpha7-containing nicotinic receptors on neurons to distal locations. European Journal of Pharmacology 2000;393:105–112. [PubMed: 10771003]

Smythe JW, Colom LV, Bland BH. The extrinsic modulation of hippocampal theta depends on the coactivation of cholinergic and GABA-ergic medial septal inputs. Neuroscience and Biobehavioral Reviews 1992;16:289–308. [PubMed: 1528522]

Thinschmidt JS, Frazier CJ, King MA, Meyer EM, Papke RL. Septal innervation regulates the function of alpha7 nicotinic receptors in CA1 hippocampal interneurons. Experimental Neurology 2005;195:342–352. [PubMed: 16000197]

Traynelis SF, Silver RA, Cull-Candy SG. Estimated conductance of glutamate receptor channels activated during EPSCs at the cerebellar mossy fiber-granule cell synapse. Neuron 1993;11:279–289. [PubMed: 7688973]

Uteshev VV, Meyer EM, Papke RL. Activation and inhibition of native neuronal alpha-bungarotoxin-sensitive nico-tinic ACh receptors. Brain Research 2002;948:33–46. [PubMed: 12383953]

Vann RE, James JR, Rosecrans JA, Robinson SE. Nicotinic receptor inactivation after acute and repeated in vivo nicotine exposures in rats. Brain Research 2006;1086:98–103. [PubMed: 16626643]

Wonnacott S, Irons J, Rapier C, Thorne B, Lunt GG. Presynaptic modulation of transmitter release by nicotinic receptors. Progress in Brain Research 1989;79:157–163. [PubMed: 2573910]

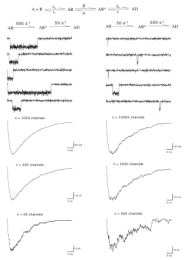

Figure 1.
Simulations of high and low P_{open} channels with linear activation schemes. The basic linear model presented at the top can be reduced to the simple three-state models below if there is rapid application of ACh to a concentration sufficiently high for all of the binding sites to be saturated. To simplify the model for the purpose of illustrating the functional equivalence of a low number of high P_{open} channels and a high number of low P_{open} channels, the rates from AR* to AR and from AD to AR* were effectively set to zero. Representative single-channel currents are shown directly below the models. Shown at bottom are summed responses of multiple channels, illustrating the similarities of magnitude and kinetics in the macroscopic currents for a low number of high P_{open} channels and a high number of low P_{open} channels

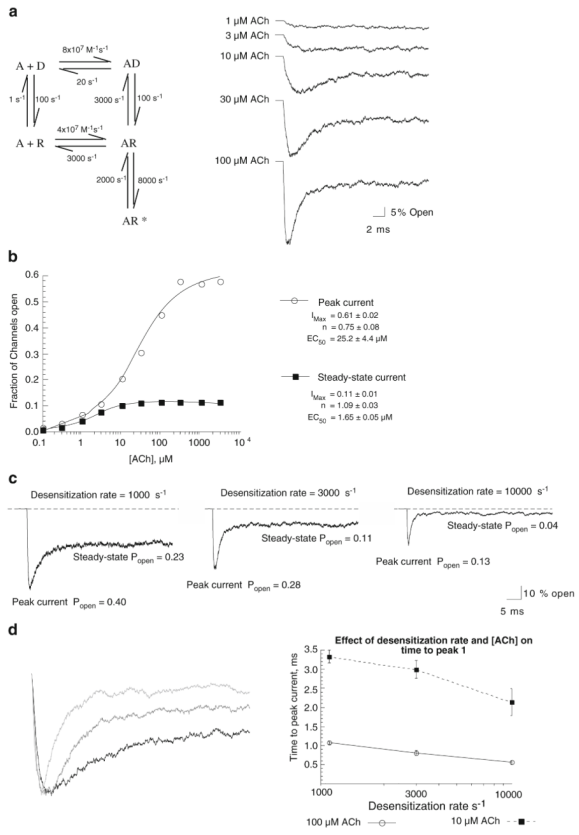

Figure 2.

Simulations of nAChR with a cyclic activation scheme. **a** A minimal model for AChR activation and desensitization (Katz and Thesleff 1957) is shown on the *left*. The model was used to generate the simulated currents shown on the *right*, representing the summed activity of 1,000 channels and the indicated ACh concentrations. For these simulations, all channels were initially in the resting R state, and the concentration of agonist was increased to the indicated values with the first 10-μs step. **b** Concentration–response curves for the multichannel simulations for both peak and steady-state currents. The steady-state P_{open} was calculated as the mean value of the final 10 ms in each simulation. Data were fit to the Hill equation (Papke and Papke 2002) to generate estimates of I_{max}, EC_{50}, and the Hill coefficient (n). **c** The effect of desensitization rates on the amplitude, time course, and magnitude of macroscopic currents. Simulations were run with the model in **a** and ACh set at 100 μM. The middle current was obtained with the initial desensitization rate (d^+) of 3,000 s^{-1}, as in **a**. The current on the left was generated with d^+ reduced to 1,000 s^{-1} and the current on the right with d^+ set at 10,000 s^{-1}. **d** Kinetic features of macroscopic currents generated with instantaneous concentration jumps and varying desensitization rates. The non-stationary portions of the currents shown in **c** are on shown the *left*. Currents with the slowest value for d^+ (1,000 s^{-1}) are in *black*, those with the intermediate rate (3,000 s^{-1}) are in *medium gray*, and those with the fastest rate (10,000 s^{-1}) are in *light gray*. For improved comparison of the rise and decay times, all currents have been scaled to the same peak amplitude. While differences in current decay times are obvious from comparisons of the scaled currents, differences in rise times are less obvious. Therefore, multiple independent simulations were run with each of the three desensitization rates and ACh set at either 100 or 10 μM. The plot on the *right* shows that time-to-peak current (averages ± SEM, n=4) was reduced when desensitization rate was increased. Note that the differences were significant

with the higher concentration of ACh ($p<0.05$) but, although the same trend is evident with the lower concentration of ACh, the differences were not statistically significant

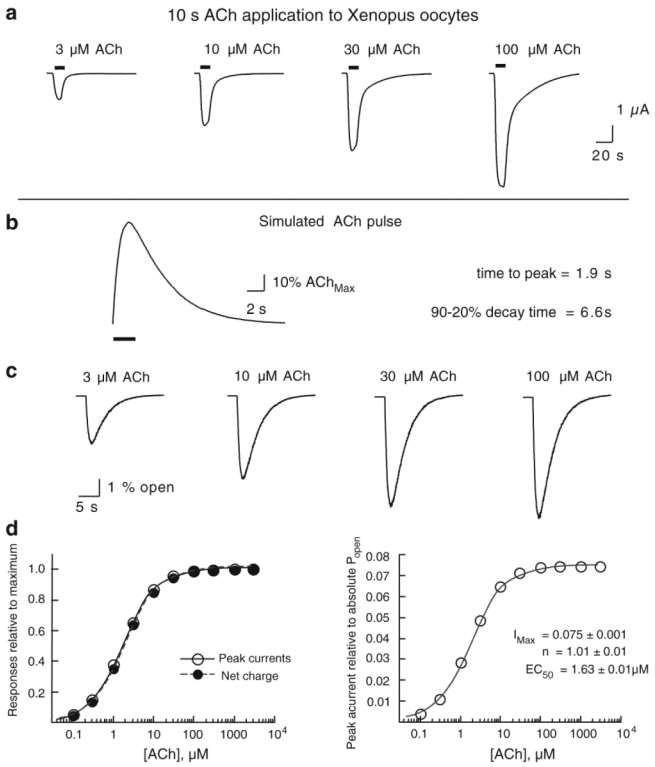

Figure 3.

Simulations of macroscopic currents in response to pulses of ACh. **a** Representative data recorded from *Xenopus* oocytes expressing human α4β2 nAChR to 10-s pulses of ACh at the concentrations indicated. **b** The pulse function used to define the time course of agonist concentration to the microscopic kinetic model in Fig. 2a. **c** Macroscopic currents for 10,000 channels to ACh pulses at the indicated concentration. **d** Concentration–response curves for the multichannel simulation for both peak currents and net charge (Papke and Papke 2002) evoked by ACh pulses. Data were fit to the Hill equation. The plots on the left were normalized to observed maximums, and on the right, the peak currents were calculated as the actual peak P_{open} values by dividing the value of the current in picoampere by 10,000, the number of channels in the simulation (each individual channel was set to conduct 1 pA when open)

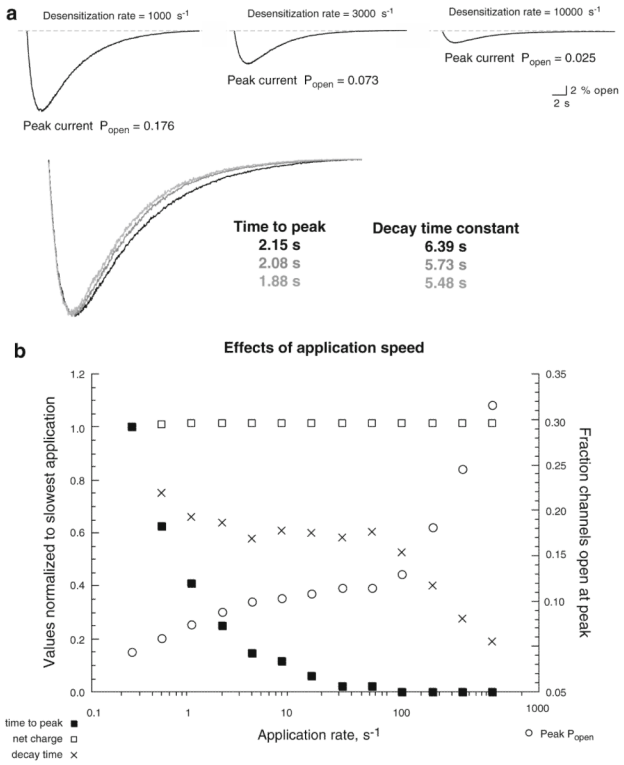

Figure 4.

The impact of desensitization and agonist application rates on macroscopic currents in response to pulses of agonist. **a** Simulations with 10,000 channels to an agonist pulse were run as in Fig. 3 but with varying values for d^+ in the underlying kinetic model. The superimposed currents shown below, scaled to the same peak amplitude, illustrate that although desensitization rates strongly impacted peak current amplitudes, they had little effect on the kinetics of the macro-scopic responses. Currents with the slowest value for d^+ (1,000 s^{-1}) are in *black*, those with the intermediate rate (3,000 s^{-1}) are in *medium gray*, and those with the fastest rate (10,000 s^{-1}) are in *light gray*. **b** The effect of application speed on macroscopic responses. Simulations were run with 10,000 channels to agonist pulses with varying rates of rise. All values for the underlying kinetic scheme were the same as in Fig. 2a, and the target ACh maximum concentration was 100 μM. Values for time to peak, net charge, and decay time were calculated relative to the respective values obtained with the slowest application onset (0.25 s^{-1}) as given on the left *Y*-axis. Peak P_{open} was calculated relative to the total number of channels in the simulation, as plotted on the right side *Y*-axis